

# Infrasonic Atmospheric Propagation Studies Using a 3-D Ray Trace Model

R. Michael Jones, Emily S. Gu<sup>1</sup>, A. J. Bedard, Jr.<sup>2</sup>

Cooperative Institute for Research in Environmental Sciences, University of Colorado, Boulder, Colorado

<sup>1</sup>Science and Technology Corporation, Boulder, Colorado

<sup>2</sup>National Oceanic and Atmospheric Administration, Environmental Technology Laboratory, Boulder, Colorado

One component of our efforts to evaluate the capabilities of a demonstration infrasonic network (ISNet) for tornado detection is to understand the impact of complex propagation paths. Although atmospheric attenuation is not significant at infrasonic frequencies (e.g.  $10^{-8}$  dB/km compared to 5 dB/km at 2 kHz), atmospheric wind and temperature gradients can have important effects upon detection ability. For example, since the early 1900s, unusual distributions of sound energy around explosions have been documented.

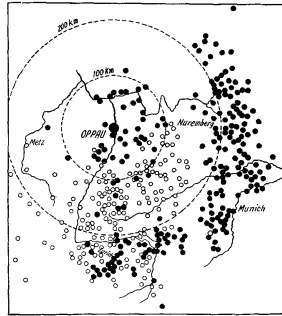


FIGURE 1. Zones of audibility and silence for the explosion at Oppau, Germany. The black dots represent places where the sound was heard, and the white circles represent places where the explosion was not heard. (After Mitra, 1952)

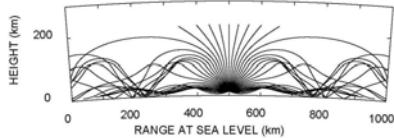


FIGURE 2. Propagation with a standard temperature profile and no wind. This is an example of a visualization of ray paths for a sound source at an altitude of 13 km for a 1962 standard atmosphere with no wind. Note that there is a gap in rays striking the surface extending to 250 km. Also note the symmetry in the two directions for sound propagating outward from the source. If rays had been launched downward (at angles  $< 20^\circ$ ), there would have been an "audible" footprint extending outward to about 20 km from the source.

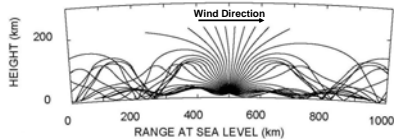


FIGURE 3. Propagation with a standard temperature profile and 5  $\text{ms}^{-1}$  wind. The climatological upper-level west-to-east wind creates asymmetry in the picture with a zone of silence from 20 to 250 km to the west and from 20 to 200 km to the east. This explains some of the basic features of the zones of audibility and silence described in figure 1.

REFERENCES  
 Jones, R. M., J. P. Riley, and T. M. Georges, 1986: HARPA -- A versatile three-dimensional Hamiltonian ray-tracing program for acoustic waves in the atmosphere above irregular terrain. NOAA Special Report, 410 pp., GovDoc No. C55.602: H 18; GPO Item No. 207-C-1; PB87132031.  
 Mitra, S. K., 1952: *The Upper Atmosphere*. The Asiatic Society, 713 pp.

- **What factors affect long-range infrasound propagation? Upper atmospheric vertical wind and temperature structure.**
- **What conditions constitute good and poor detectability at the earth's surface for shorter ranges? Tropospheric vertical wind and temperature gradients.**
- **What factors can produce bearing errors? Horizontal wind and temperature gradients.**
- **How do these factors impact the design of infrasound networks? Indicates that denser networks are required for complete detection, especially for key locations (e.g. along urban corridors).**

To answer these questions, we applied a three-dimensional acoustic ray-tracing program (Jones, Riley, and Georges, 1986). The ray-tracing program traces the three-dimensional paths of acoustic rays through model atmospheres by numerically integrating Hamilton's equations, which are a differential expression of Fermat's principle. We examined a series of idealized and realistic cases in the process of addressing these questions, including isothermal layers, thermal inversions, and Gaussian wind jets. Our future plans include modeling propagation for landspout and supercell environments.

Situation	Region Near Source	Distant No Wind	Distant Upwind	Distant Downwind	Comments
Standard atmosphere & no wind	$\pm 20$ km	20 to 200 km symmetric zones of silence			
Standard atmosphere & upper level wind	$\pm 20$ km		20 to 250 km zone of silence	100 to 200 km zone of silence	Distant upwind propagation weak at long ranges
Inversion & isothermal lower layer	No zone of silence	No zone of silence	No zone of silence	No zone of silence	
Source at center of mesocyclone					Ray rotation, but no bearing errors
Source 20 km south of mesocyclone					Bearing errors only for rays passing through mesocyclone core
Low-level Gaussian wind field of 10 $\text{ms}^{-1}$			Upward refraction produces zones of silence	No zone of silence	

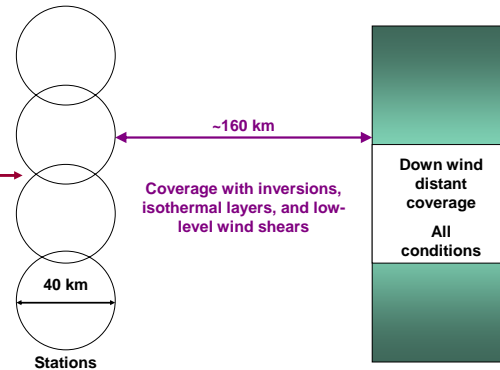


FIGURE 4. An Urban Corridor Net Concept

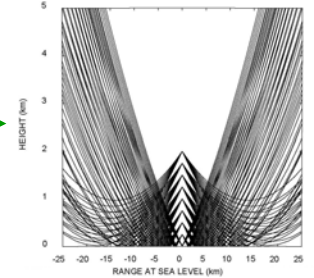


FIGURE 6. Propagation with a standard temperature profile, no wind, and a transmitter fan array. This source model assumes an isotropically radiating distributed source using discrete sources located from the surface to 2 km at 250 m intervals. This ray-trace visualization shows robust propagation out to approximately 20 km.

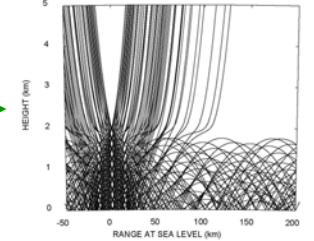


FIGURE 7. Propagation with a thermal inversion at 2 km, isothermal below 2 km, no wind, and a transmitter fan array. The significant features of this case are a low level thermal inversion at 2 km and an isothermal region below 2 km. There are multiple transmitters, equally spaced between 0 and 2 km at 250 m intervals. Rays are launched from an azimuth angle of  $90^\circ$  and from elevation angles ranging from  $-5^\circ$  to  $5^\circ$  in  $1^\circ$  increments. It can be seen that the temperature inversion bends sound rays back towards the earth, allowing for detection virtually anywhere horizontally from the transmitter out to 200 km and beyond. The isothermal nature of this case allows for the rays to continue downward and reflect off the earth's surface. It is such fine-scale temperature or wind structure that creates variety in the ray paths of sound propagation.

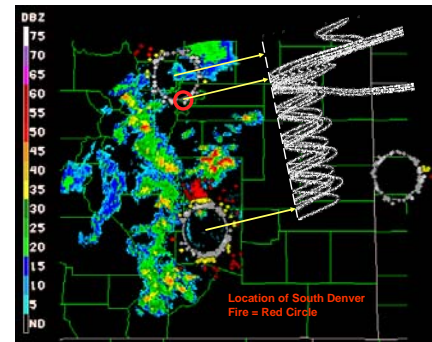


FIGURE 5. ISNet image showing Pueblo's robust detection of the July 19, 2003 fire, and the BAO's lack of detection due to a lower-level wind field moving north-to-south. We simulated the low-level flow as a Gaussian wind field of  $10 \text{ ms}^{-1}$  centered at 3 km. The ray paths shown indicate that these winds were critical to the detection at Pueblo and the lack of signal at Boulder even though the BAO is much closer than Pueblo (30 km versus 175 km, respectively). There was no significant inversion present for this case.

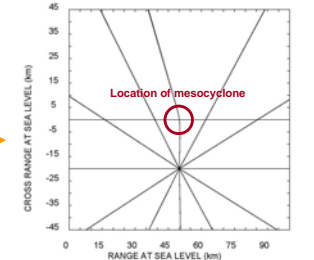


FIGURE 8. Propagation through a mesocyclone. We simulated a mesocyclone as a counter-clockwise rotating Rankin-combined vortex with a maximum tangential wind speed of  $20 \text{ ms}^{-1}$  at a radius of 5 km. Rays are presented in a horizontal plane with a tomographic source located 20 km to the south of the mesocyclone. Only rays passing directly through the vortex are bent.